Adsorbed Hydrogen Effect on the Adsorption and Reactivity of N_2 Molecules on Ru/MgO and Ru–Cs^+/MgO: Hydrogen Dipole Effect Enhanced by Doped Cs^+

Yasuo IZUMI,* Masaki HOSHIKAWA, and Ken-ichi AIKA*
Department of Environmental Chemistry and Engineering, Interdisciplinary Graduate School of Science and Engineering, Tokyo Institute of Technology, 4259 Nagatsuta, Midori-ku, Yokohama 227

(Received June 28, 1994)

The effects of adsorbed hydrogen on the N_2 adsorption and N_2 isotope displacement rate on Ru/MgO and Ru–Cs^+/MgO were investigated by FTIR. The H_2 was found to be adsorbed dissociatively on on-top sites [1880w(sh), 1801w(sh), and 1717s cm^{-1}], bridging sites [1550w and 1330w cm^{-1}], and threefold sites [1120m and 933m cm^{-1}] on Ru/MgO, and similarly on three kinds of adsorption sites on Ru–Cs^+/MgO. The bridging hydrogen on Ru/MgO was thermally more stable than the other two. Molecular N_2 could be adsorbed as an on-top form on Ru. By the small amount of preadsorbed H(a) [$H(a)/Ru_{surf}=14\%$], the N_2 isotope displacement rate $^{15}N_2(a)\rightarrow{}^{14}N_2(a)$ in $^{14}N_2$ on Ru/MgO was largely reduced to 12%, and the reduction on Ru–Cs^+/MgO was more serious (to 4%). The main factors of these reductions were interpreted as direct repulsion of H(a) and N_2 on Ru/MgO and Ru-hydride dipole effect enhanced by doped Cs^+ on Ru–Cs^+/MgO. The common factors in N_2 displacement reaction and the catalysis from N_2 are discussed in terms of the hydrogen effect.

Recent developments in spectroscopy have opened the door to new information about the surface intermediate species during catalysis and their detailed behavior.[1] Ruthenium is widely known to be applicable for ammonia synthesis,[2,3] FT synthesis,[4] and partial hydrogenation of benzene.[5] Spectroscopic studies on Ru(0001) single crystal surfaces have revealed important information such as regular disposition of adsorbed N_2,[6] H,[7] CO,[8] coadsorbed N_2 with O or K,[6] CO with NH_3,[9] adsorption sites of H,[7,10—14] or Ru surface relaxation.[10]

Hydrogen atoms have been reported to be adsorbed on the threefold sites of the Ru(0001) face.[7,10—14] Adsorbed H forms ordered structures: $p(\sqrt{3}\times\sqrt{3})$ R30° at $\theta_H=33\%$, $p(2\times1)$ at $\theta_H=50\%$, $(2\times2)-3H$ at $\theta_H=75\%$, and 1×1 at $\theta_H=100\%$.[7] With the increase of the amount of adsorbed hydrogen from 0 to ca. 10 L (1 L=0.133 kPa s) on Ru(0001) at 173 K, the work function (ϕ) first increased to +25 meV (maximum at $\theta_H\approx50\%$) and then linearly decreased.[12] This irregular work function change was interpreted as due to the sum of two surface dipole moments at H(a), μ_P (outward perpendicular to the surface) and μ_N (inward perpendicular to the surface). A small β_1 peak of H(a) which was weakly-bound and was desorbed around 330 K in TPD (temperature programmed desorption) roughly corresponded to the outward dipole, and a subsequent large peak β_2 desorbed at 360—440 K roughly corresponded to the inward dipole. The adsorption site of $p(2\times1)$H on Ru(0001) has been suggested to be the threefold fcc site rather than on-top, bridging, threefold hcp, or sublayer sites[15] by the curve-fitting analysis for energy dependence (20—220 eV) of diffraction intensity of the LEED (low-energy electron diffraction).[10] In the curve-fitting procedure, Ru surface layer(s) reconstruction was included as changeable parameters along with the parameters for the position of adsorbed H. The change of distance between first and second Ru-layers was suggested to be the reason for the irregular work function change. The height of H(a) from the first Ru layer may decide the direction of the surface dipole moment.[10]

Nitrogen adsorption on Ru(0001) has been also studied.[6,16] The ordered structure of $p(\sqrt{3}\times\sqrt{3})$ R30°-N_2 at $\theta_{N2}=33\%$ is known, and repulsive interaction of K and N_2 has been examined by EELS (electron energy loss spectroscopy), UPS (ultraviolet photoelectron spectroscopy), TPD, and the change of work function ($\Delta\phi$). The minimum K–N_2 interaction distance has been estimated to be about $\sqrt{3}r_{Ru-Ru}$ (r_{Ru-Ru}: Ru–Ru bonding distance).[6] Two chemisorbed states δ and γ have been observed at 78 K, which were desorbed at 88 and 115 K, respectively.

In the viewpoint of ammonia synthesis on Ru, hydrogen plays complex roles.[17] The reaction rate of ammonia synthesis can be expressed as follows in the case of Fe and Ru:

$$r = kP_{N2}(P_{H2}{}^3/P_{NH3}{}^2)^{0.5} \quad \text{(on Fe catalysts)}^{3)}$$

$$r = kP_{N2}P_{H2}{}^{0.5}P_{NH3}{}^{-0.8} \quad \text{(on Ru catalysts)}^{18)}$$

$$r = kP_{N2}P_{H2}{}^{-0.5}P_{NH3}{}^{0} \quad \text{(on alkali-doped Ru catalysts)}^{18)}$$

Considering the inhibition term in the Langmuir equation, these rate expressions suggest that the metal surface of the Ru or alkali-doped Ru catalysts is covered by more amount of H(a) than in the case of Fe catalysts.[18] This tendency that hydrogen dominantly occupied Ru surface site was more prominent when Ru catalyst was doped with alkali metal K, Na, or Cs (the dependence on P_{H2} was minus (ca. −0.5)). The simplest understanding of the role of alkali metal is the partial electron donation to the metal surface to make the electron-rich environment to facilitate the rate-limiting dissociation step of N_2 to N(a), and at the same time, to make H(a) more negative and stabilized. Indeed, Cs^+ doped

to Ru/Al_2O_3 promoted the rate of ammonia synthesis quite effectively in ambient pressure, but the rate did not increase so much with the increase of total reaction gas pressure, unlike the monotonous increase on industrial Fe catalysts, because the amount and blocking effect of H(a) would be more serious at higher pressures. However, to our surprise, the ammonia synthesis rate was rather accelerated according to the increase of reaction gas pressure when rare-earth metal such as Ce or Sm was doped in Ru/Al_2O_3,[19] or on $[Ru_3(\mu\text{-}O_s)_3]$-derived clusters on CeO_2 (the structure was determined by EXAFS).[20] Thus, the adsorbed state of H(a) on the Ru catalyst should be studied in relation to the N_2 activation.

This paper is intended to fill the gap between catalysis on the most active Cs^+-doped Ru/MgO[21] and adsorption results for H(a) and N_2(a) on catalyst surfaces. We reported ν_{RuH} peak of H(a) (on-top, bridging)[22] and ν_{NN} peak of N_2(a)[23] on Ru/MgO, Ru–Cs^+/MgO, Ru/Al_2O_3, or Ru–Cs^+/Al_2O_3. Considering the stable Ru(0001) face and fewer coordinately-unoccupied Ru sites (edge sites) on our Ru particle (average diameter of 2.6 nm) on MgO, the N_2 displacement and the N_2 adsorption rates were followed on a H-free and H-preadsorbed Ru/MgO (θ_H=14—89%) and on a Ru–Cs^+/MgO catalyst (θ_H=0—50%). The changes of adsorbed amount and the wavenumber of ν_{NN} peak for N_2 were also measured, and the effects of H(a) were classified to (1) direct repulsion and (2) long-range dipole effect. The change of dipole effect of H(a) by doped Cs^+ is discussed by comparing the results on Ru/MgO and Ru–Cs^+/MgO.

Experimental

FTIR spectra (JASCO FTIR5300) were obtained for the disk samples in a quartz cell equipped with NaCl windows on both sides which was connected to closed circulation system. The preparation procedures of catalysts were described previously.[21] Briefly, the solution of $Ru_3(CO)_{12}$ in tetrahydrofuran was reacted in air with MgO (130 $m^2 g^{-1}$) (Ru 2 wt%), followed by evaporation of the solvent, H_2-reduction at 773 K (12 h), and evacuation at 773 K (1 h) (Ru/MgO). MgO was impregnated with $CsNO_3$ in water solution, which was decomposed under O_2 (2 h) and H_2 (48 h) atmosphere at 773 K. The obtained sample Cs^+/MgO was impregnated with $Ru_3(CO)_{12}$ in the same way as MgO giving Ru–Cs^+/MgO (Cs/Ru=2.0 in atomic ratio). Measured amounts (about 0.1 g) of thus-prepared catalysts were pressed to disks (ϕ=20 mm). Before each measurement, each sample disk was again treated in H_2 (773 K, 1 h) and evacuated (773 K, 1 h). The electron microscope measurements indicated that once formed Ru particles with an average diameter ($2d$) of 2.6 nm on MgO by the 12 h-reduction showed no further significant change of particle size by the subsequent treatment in H_2.

The dispersion (D) of Ru particle was estimated from the equation:

$$D = \frac{4\pi d^2/(\sqrt{3}/2){r_{Ru-Ru}}^2}{(4/3)\pi d^3 \rho N_A/MW} = \frac{1.30}{2d/nm}$$

with the Avogadro number (N_A), molecular weight of Ru (MW), the density of Ru ρ (12.36 $g\,cm^{-3}$) and the r_{Ru-Ru} (0.270 nm). D was 0.50 when $2d$ was 2.6 nm. This Ru dispersion and hydrogen uptake measurement indicated a 1 : 1 ratio of H/Ru_{surf} on Ru/MgO. In the estimation of IR peak area, peak deconvolution were carried out by the non-linear least square fitting method with Gaussian functions (Fig. 1). The correlations between IR peak intensity and the amount of adsorbate in mol (estimation of ε_H and ε_{N2}) were obtained by the estimation of desorbed H_2 (49 and 36 $\mu mol\,g_{cat}^{-1}$ for Ru/MgO and Ru–Cs^+/MgO, respectively) or N_2 (37 and 16 $\mu mol\,g_{cat}^{-1}$ for Ru/MgO and Ru–Cs^+/MgO, respectively) according to the decrease of ν_{RuH} or ν_{NN} peaks. The difference of total hydrogen uptake monitored by a manometer and that obtained from IR peak of H(a) on Ru particle was allotted to the increased intensity of ν_{OH} peak on MgO surface (ε_{OH}).

6.7 kPa of hydrogen was introduced to the IR cell in which the in-situ pretreated disk of Ru/MgO was placed at 183 K. Subsequently gas phase H_2 was evacuated, and the temperature was elevated. At 293, 473, and 548 K or 293, 373, and 523 K, temperature elevation was temporarily stopped during the data scanning.

The rates of isotope displacement reactions were observed by introducing 1.5 kPa of $^{14}N_2$ to $^{15}N_2$-preadsorbed Ru/MgO at 183 K. The initial rate of ν_{NN} peak shift from 2083 cm^{-1} of $^{15}N_2$(a) to 2154 cm^{-1} of $^{14}N_2$(a) was followed on Ru/MgO and the shifts (2048 and 1950→2120 and 2020 cm^{-1}) were followed on Ru–Cs^+/MgO by observing the increase of peak area of $^{14}N_2$(a) after peak deconvolution. The same measurements were carried out on H-preadsorbed catalysts at θ_H=0, 14, 36, and 65% for Ru/MgO and at θ_H=0, 14 and 50% for Ru–Cs^+/MgO. In order to vary the θ_H in small degrees, the H_2 adsorption temperatures were changed, and also in some runs, H_2 gas (0.13—6.7 kPa) was added to $^{14}N_2$ so as to increase θ_H. Isotope equilibration reaction $^{15}N_2+{}^{14}N_2 \rightarrow 2{}^{14}N^{15}N$ was monitored by a mass spectrometer with 10 kPa of $^{15}N_2$ and 10 kPa of $^{14}N_2$ at 548 K. The rate of ammonia synthesis was also measured in 25.3 kPa of N_2 and 76.0 kPa of H_2 at 548 K. The increase of ν_{OH} mode of hydroxyl group on MgO in H_2 was monitored as the amount of spillover hydrogen from Ru metal particles to MgO surface at 183—473 K.

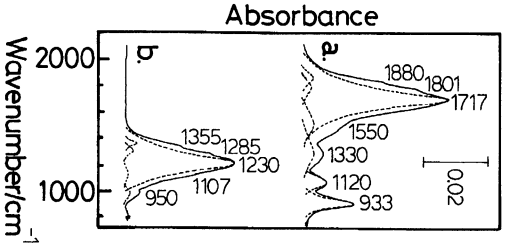

Fig. 1. The peak deconvolution by Gaussian functions of IR spectra of Ru/MgO (Ru 2 wt%) at 293 K under 6.7 kPa of H_2 (a) and corresponding deconvoluted spectrum under 6.7 kPa of D_2 (b).

Results

Hydrogen Adsorption on Ru/MgO. When hydrogen was introduced on Ru/MgO at 183 K, a strong main peak was observed at 1717s cm^{-1} [Fig. 2(a)] with weaker peaks at 1880w(sh), 1801w(sh), 1550w, 1330w, 1120m, and 933m cm^{-1}. In 6.7 kPa of H_2 at 293 K the spectrum was essentially the same, except that peaks at 1880 and 1801 cm^{-1} were weaker [Fig. 1(a)]. Peaks observed in D_2 (6.7 kPa, 293 K) at 1355w(sh), 1285w(sh), 1230s, 1107w, and 950w cm^{-1} [Fig. 1(b)] corresponded to peaks in H_2 at 1880w(sh), 1801w(sh), 1717s, 1550w, and 1330w cm^{-1}, respectively [Fig. 1(a)]. Because of the strong absorption by the support MgO, no shifted peaks in D_2 corresponding to those in H_2 at 1120 and 933 cm^{-1} were detected.

We assigned the peaks at 1880, 1801, and 1717 cm^{-1} to on-top H. The stretching mode for μ_1-H of transition metal hydride complexes[24,25] and the H(a) on supported transition metal catalysts[26—29] were reported to be at 2250—1700 cm^{-1} (Table 1). As the peaks at 1880 and 1801 cm^{-1} were only observed at 183 K [Fig. 2-(a)], they may be twin-type H(a). The EELS spectra of adsorbed hydrogen on Ru(0001) surface have been reported at 1113 (ν_{as}) and 847 (ν_s) cm^{-1} at 180 K, which were shifted in D_2 to 831 and 540 cm^{-1},[13] or at 1137 and 823 cm^{-1} at 105 K [Table 1(a)].[14] As only threefold H has been reported on Ru(0001) surface[7,10—14] our IR peaks at 1120m and 933m cm^{-1} can be assigned

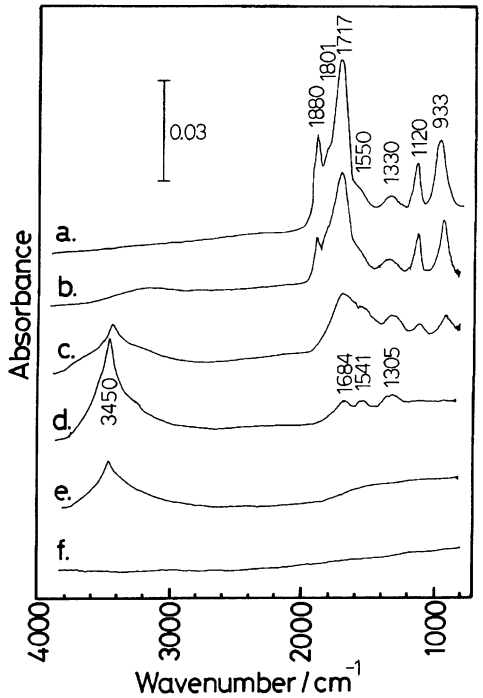

Fig. 2. The IR spectra of adsorbed hydrogen on Ru/MgO (Ru 2 wt%) at 183 K under 6.7 kPa of H_2 (a), after the evacuation at 183 (b), 293 (c), 473 (d), and 548 K (e). Hydrogen was not adsorbed on MgO at 183 K in 6.7 kPa of H_2 (f).

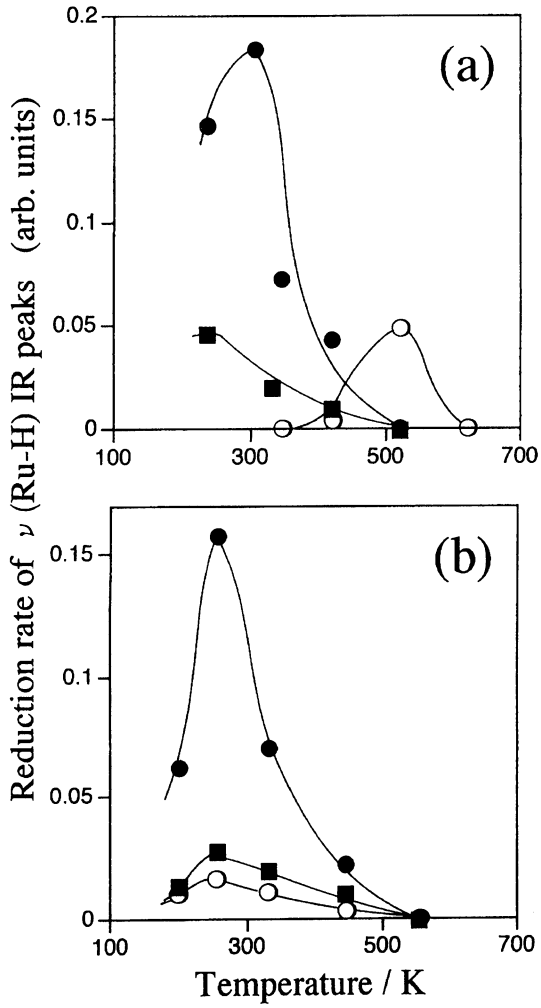

Fig. 3. The reduction rate of IR peak for adsorbed hydrogen on Ru/MgO (a) and Ru–Cs^+/MgO (b) as a function of the temperature; ●: on-top, ○: bridging, ■: threefold. The heating rate was 4 K min^{-1}.

to threefold H on Ru particles. The blue-shifts of 83—110 cm^{-1} for ν_s mode from EELS data would be due to the modification of the symmetry of H(a) to change the energy gap of ν_{as} and ν_s and also to the electronic modification of ruthenium particles by support MgO.[21] Vibrational data for other threefold H on Ru_6 cluster[30] or metal single crystals[31,32] were reported [ν=1230—550 cm^{-1}, Table 1(a)]. These two peaks (ν_{as} and ν_s) were desorbed while keeping the intensity ratio when heated in vacuum [Fig. 2(b)—(e)]. The two peaks at 1550 and 1330 cm^{-1} can be assigned to ν_{as} and ν_s of bridging H(a), respectively, when we consider the wavenumbers of on-top and threefold H(a) assigned above and the bridging H of organometallic hydride Ru_4 cluster (1585, 1290 cm^{-1}).[25,33] These two peaks (ν_{as} and ν_s) were desorbed, also while keeping the intensity ratio when heated [Fig. 2(b)—(e)]. 6.7 kPa of H_2 was introduced at 183 K to MgO disk sample pretreated in H_2, and this was evacuated at 773 K. No adsorption peak was observed [Fig. 2(f)].

Table 1. Vibrational Spectroscopic Data for H-Metal Complexes or Clusters(a) and Adsorbed H(a) or N_2(b) on Metal Single Crystals or Supported Metal Catalysts

Sample	Gas	T_{ad}/K	ν_{RuH}/cm^{-1}			Method	Ref.
			On-top	Bridging	Threefold		
(a) H							
$H_2Ru(CO)_4$	—	—	1980			IR	25
$H_2Ru(CO)_2(PPh_3)_2$		—	1878, 1823			IR	25
Fe–Al_2O_3–K_2O	101 kPa	R.T.	1954, 1902, 1870			Raman	26
[HRh(μ-O_s)$_2$]/TiO_2	—	—	2048			FTIR	27
Rh/Al_2O_3	10^3 kPa	298	2013			FTIR	28
Fe, Co, Ni, Rh, Pd, and Ir/Al_2O_3	—	—	1940—1850			IR	29
$H_4Ru_4(CO)_{12}$	—	—		1585, 1290		Raman	33
$H_4Ru_4(CO)_{12}$	—	—		1284		IR	25
$H_2Ru_6(CO)_{18}$	—	—			708, 660, 652	FTIR	30
Ru(0001)	Saturated	180			1113, 847	EELS	13
Ru(0001)	Saturated	105			1137, 823	EELS	14
Ru(110)	—	—			1136, 1031, 685	EELS	31
Pd(111)	2 L[a)]	120			998, 773	EELS	31
Pt(111)	60 L	90			1230, 550	EELS	32
Ru/MgO	6.7 kPa	173	1870m(sh), 1760s	1330m		FTIR	22
Ru/MgO	6.7 kPa	183	1880w(sh), 1801w(sh), 1717s	1550w(sh), 1330w	1120m, 933m	FTIR	This work
Ru–Cs^+/MgO (Cs/Ru=2)	6.7 kPa	183	1781s	1540w(sh), 1407w	1233m, 940m	FTIR	This work

(b) N_2 (on-top)

Sample	Gas	T_{ad}/K	ν_{NN}/cm^{-1}	Method	Ref.
Ru(0001)	23 L[a)]	40	2331m(sh), 2194s	EELS	16
Ru(0001)	4 L	78	2189	IRAS	6
Ru(0001)	Saturated	85	2195	EELS	6
K–Ru(0001) (θ_K=0.05)	Saturated	85	2150	EELS	6
O–Ru(0001) (θ_O=0.25)	Saturated	85	2239	IRAS	6
O–Ru(0001) (θ_O=0.5)	Saturated	85	2250	EELS	6
Ru/MgO	6.7 kPa	160	2168s, 2100m(br)	FTIR	23
Ru–Cs^+/MgO(Cs/Ru=1)	6.7 kPa	160	2070m(br), 1910m	FTIR	23
Ru/MgO	6.7 kPa	183	2154	FTIR	This work
Ru–Cs^+/MgO(Cs/Ru=2)	6.7 kPa	183	2120s, 2020s(sh)	FTIR	This work

a) 1 L=0.133×10^{-6} kPa s.

By the evacuation of gas-phase H_2 at 183 K, the on-top (1717 cm^{-1}) and threefold (1120 cm^{-1}) peaks decreased, but the peak intensity at 1330 cm^{-1} (bridging) was not changed. In Fig. 3(a), on-top and bridging H were desorbed around 280 and 500 K, respectively. Compared to the desorption temperature of threefold H on Ru(0001) (β_1: 330 K, β_2: 360—440 K),[11] the TPD peaks of on-top site H and threefold H on Ru/MgO were within the comparable range. On the other hand, the remarkable stability of bridging H (ca. 500 K) suggested that the bridging H was located on the lower-coordination (LC) Ru site (edge site), in contrast to the on-top and the threefold H, which were located on the relatively flat surface of Ru particles.

Nitrogen Adsorption on Ru/MgO. Nitrogen was molecularly adsorbed on Ru/MgO, giving a peak at 2154 cm^{-1}, as shown in Fig. 4(a). This peak can be assigned to ν_{NN} of linear N_2 on on-top site, red-shifted by 45 cm^{-1} from full coverage N_2(a) (2189 cm^{-1}; θ_{N2}=33%) on Ru(0001)[6] by the backdonation effect due to basic MgO.

The influence of adsorbed hydrogen to the peak intensity and wavenumber of N_2(a) was examined by the ν_{NN} peak observation in N_2 (183 K) without H_2 adsorption [Fig. 4(a)], with hydrogen chemisorbed (gas-phase H_2 was evacuated) at 473, 293, and 183 K [Fig. 4(b), (c), and (d), respectively] or with 0.67 kPa of H_2 at 183 K [Fig. 4(e)]. Based on peak deconvolution (Fig. 1), total peak area of H(a) was 14% for Fig. 4(b), 36% for (c), 65% for (d), and 89% for (e) compared to Fig. 2-

Table 2. (a) The Intensities of H(a) and N_2(a) Peaks, and the Rates of (b) Isotope Displacement Reaction, (c) Isotope Equilibration Reaction, and (d) Ammonia Synthesis Reaction on Ru/MgO

Entry	I	II	III	IV	V	VI	VII	VIII	IX	X
H_2 adsorption T/K	183			293		473		548	no H[a]	
H_2/kPa	6.7	1.3	0	1.3	0	1.3	0	0		
	θ/%									
(a) θ_H	100		65		36		14	0		
θ_{N_2}[b]			8.0		25		38	38		
	r/μmolg^{-1}s^{-1}									
(b) $^{15}N_2(a) \rightarrow {}^{14}N_2(a)$[b]			0.53		0.6		1.3		11	
(b′) $N_2(g) \rightarrow N_2(a)$[b]							37		45	
(c) $^{15}N_2(a) + {}^{14}N_2 \rightarrow 2{}^{14}N{}^{15}N$[c]									0.0033	
(d) $N_2 + 3H_2 \rightarrow 2NH_3$[d]										0.0024

a) H_2 was not introduced. b) P_{N_2}=1.5 kPa at 183 K. c) P_{N_2}=20 kPa of N_2 at 548 K. d) P_{N_2}=25 kPa, P_{H_2}=76 kPa at 548 K.

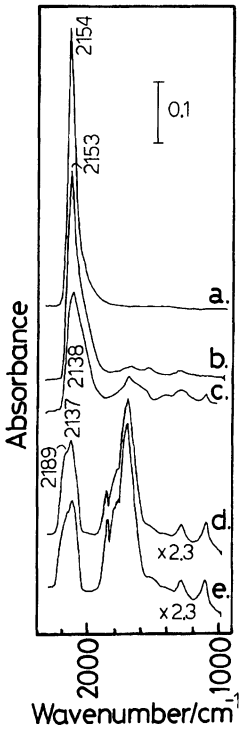

Fig. 4. The change of IR peaks of adsorbed N_2 on Ru/MgO in 6.7 kPa of N_2 as a function of the coverage of previously adsorbed H (a); H_2 was not introduced (a). H_2 was introduced and evacuated at 473 (b), 293 (c), and 183 K (d). 0.67 kPa of H_2 was introduced at 183 K (e).

(a) (100%) (H_2 6.7 kPa, 183 K) [Table 2(a)]. While the wavenumber of ν_{NN} peak gradually shifted to the low-energy side: 2154 [Fig. 4(a)] → 2153 [Fig. 4(b)] → 2138 cm^{-1} [Fig. 4(c)] according to the decrease of the amount of N_2(a), a new peak of ν_{NN} appeared at 2189 cm^{-1} as a shoulder of the peak of 2137 cm^{-1} with a large increase of preadsorbed hydrogen up to θ_H=65% (183 K) [Fig. 4(d), Table 3]. Further increase of θ_H to 89% reduced total peak area of ν_{NN}, but the ratio

Table 3. The Wavenumber of ν_{NN} (cm^{-1}) of Adsorbed N_2 on Ru/MgO or Ru–Cs^+/MgO with the Function of Hydrogen Coverage

(a) Ru/MgO

Ru θ_H/%					
0	14	36	65	89	100
2154s	2153s	2138s	2189m 2137m	2190m 2136m	ND

(b) Ru–Cs^+/MgO

θ_H/%			
0	14	50	100
2120s 2020s(sh)	2118w(sh) 2026s	2120w 2020w	ND

ND: not adsorbed.

of the two and the wavenumbers showed no significant difference [Fig. 4(e) and Table 3(a)]. With regard to the initial shift to low frequency with the decrease of N_2 amount in Fig. 4(a)—(c) (with the increase of θ_H preadsorbed), the following experiment was added. We gradually decreased θ_{N_2} from 38 to 1.1% by changing the N_2 gas amount under H-free condition, and found that the ν_{NN} peak also gradually red-shifted (from 2154 to 2106 cm^{-1}). This shift was contrary to the reported blue-shift of N_2 on Ru(0001).[6]

The correlations between the amount of preadsorbed H and that of N_2 (chemisorbed+physisorbed or chemisorbed only) at 183 K are shown in Fig. 5 (solid lines). The first adsorption was regarded as chemisorption+physisorption, and subsequent uptake after the evacuation for 5 min was regarded as physisorption. The estimation of N_2(a) by gas chromatography for the Ru/MgO powder indicated that the fully chemisorbed N_2 (at θ_H=0) was 31% of the surface Ru. Although the steep reduction curve of the amount of chemisorbed N_2 implied that one hydrogen atom blocked two or more adsorption sites of N_2, the total

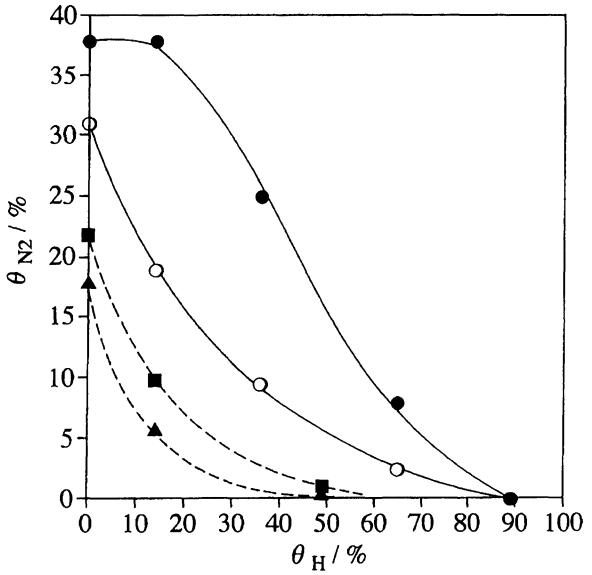

Fig. 5. The change of the adsorbed amount of N_2 as a function of preadsorbed total amount of H on Ru/MgO (solid line) and on Ru–Cs^+/MgO (dotted line); ●, ■: physisorbed+chemisorbed N_2 ○, ▲: chemisorbed N_2.

(=chemisorbed+physisorbed) amount decreased moderately, suggesting that adsorption of physisorbed N_2 is controlled by some factors.

Dependence of N_2 Isotope Displacement Rate on the Amount of H(a) for Ru/MgO. The substitution reaction rates of $^{15}N_2$(a) (2083 cm^{-1}) for $^{14}N_2$ (2154 cm^{-1}) were observed at 183 K on Ru/MgO or H-preadsorbed Ru/MgO (H_2 adsorption temperature: 183, 293, 473 K). The rates with chemisorbed H (θ_H=14—65%) were 5—12% (0.53—1.3 $\mu molg^{-1}s^{-1}$) of that without H(a) (11 $\mu molg^{-1}s^{-1}$) [Table 2(b)]. A very small amount of H adsorbed (θ_H<14%) retarded molecular N_2 displacement reaction in the order of one. The adsorption rate of N_2 was also observed by FTIR at 183 K on H-free catalyst sample and that with θ_H=14% (without preadsorbed N_2). The observed rates [45 and 37 $\mu molg^{-1}s^{-1}$, respectively; Table 2(b′)] were faster than N_2 displacement reaction [11 and 1.3 $\mu molg^{-1}s^{-1}$, respectively; Table 2(b)] under the same conditions.

The Effect of H(a) on the Reactivity of N_2(a) on Ru–Cs^+/MgO. 6.7 kPa of H_2 was adsorbed on Ru–Cs^+/MgO at 183 K in the same manner as on Ru/MgO. The main on-top H peak on Ru–Cs^+/MgO [Fig. 6(a)] was quite weak compared to that on Ru/MgO at 183 K [Fig. 2(a)], but at 293 K in 6.7 kPa of H_2, the total H peak area [Fig. 6(b)] became comparable to Fig. 2(a) (73% of that on Ru/MgO at 183 K on g-cat basis). In the estimation of Ru_{surf} on Ru–Cs^+/MgO, this peak intensity and H_2 uptake measurement at 293 K (36 $\mu mol\,g_{cat}{}^{-1}$-H_2) were taken as standard (=100%). The five peaks observed at 1781s, 1540w, 1407w, 1233m, and 940m cm^{-1}, blue-shifted from those on Ru/MgO due to further electron donation by Cs^+ than only by MgO,

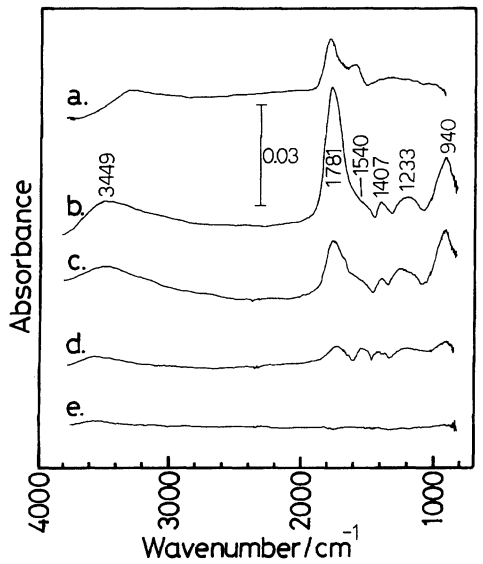

Fig. 6. The IR spectra of adsorbed hydrogen on Ru–Cs^+/MgO (Ru 2 wt%, Cs/Ru=2.0 in atomic ratio) at 183 (a) and 293 K (b) in 6.7 kPa of H_2, evacuated at 293 (c), 373 (d), and 523 K (e).

were assigned to on-top, ν_{as} and ν_s of bridging, and ν_{as} and ν_s of threefold H, respectively. When we elevated the temperature, each adsorbed H peak decreased [Fig. 6(c), (d)]. All three kinds of H desorbed around (or less than) 340 K [Fig. 3(b)].

In N_2 at 183 K on Ru–Cs^+/MgO, the strong single peak at 2154 cm^{-1} on Ru/MgO [Fig. 4(a)] shifted and split to 2120s and 2020s(sh) cm^{-1} [Fig. 7(a)]. The θ_{N2} on H-free Ru–Cs^+/MgO was 57% [Tables 3(a) and 4(a)] of θ_{N2} on H-free Ru/MgO. The adsorbed N_2 at 2020 cm^{-1} must be more influenced by Cs^+ to be

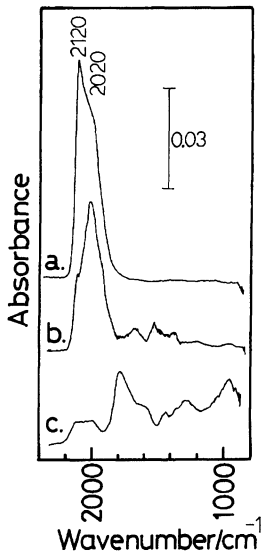

Fig. 7. The change of IR ν_{NN} peaks of adsorbed N_2 on Ru–Cs^+/MgO in 6.7 kPa of N_2 at 293 K as a function of the coverage of previously adsorbed H(a); H_2 was not introduced (a), H_2 was introduced and evacuated at 373 (b), 293 K (c).

Table 4. (a) The Intensities of H(a) and N_2(a) Peaks, and the Rates of (b) Isotope Displacement Reaction, (c) Isotope Equilibration Reaction, and (d) Ammonia Synthesis Reaction on Ru–Cs^+/MgO

Entry	I	II	III	IV	V	VI	VII
H_2 adsorption T/K	293			373	523	no H[a)]	
H_2/kPa	6.7	1.3	0	0	0		
	θ/%						
(a) θ_H	100		50	14	0		
θ_{N_2}[b)]	0		1.3	10	22		
	r/μmolg^{-1} s^{-1}						
(b) $^{15}N_2$(a)→$^{14}N_2$(a)[b)]				0.48		11	
(b′) N_2(g)→N_2(a)[b)]				8.5		50	
(c) $^{15}N_2$(a)+$^{14}N_2$→$2^{14}N^{15}N$[c)]						0.029	
(d) N_2+3H_2→$2NH_3$[d)]							0.039

a)—d) Footnotes are the same as in Table 2.

red-shifted by 134 cm^{-1} from 2154 cm^{-1} for N_2 on Ru/MgO. Another peak at 2120 cm^{-1} was less affected (Δ=34 cm^{-1}), but the effect was still comparable to $\Delta\nu_{NN}$ for N_2 on metallic K–Ru(0001) (Δ=45 cm^{-1}) [Table 1(b)].[6] The former Ru site should be located nearer to the Cs^+ part.

The influence of preadsorbed hydrogen on the peak intensity of N_2(a) was more serious on Ru–Cs^+/MgO [Fig. 7(b), (c)]. Lower wavenumber peak at 2026 cm^{-1} became dominant at θ_H=14% [Fig. 7(b)]. At θ_H=50%, two very weak peaks were observed [Fig. 7(c)]. This can be interpreted that, at higher θ_H, greater percentage of N_2 was forced to be adsorbed on the Ru site nearer to Cs^+. The amounts of chemisorbed or total N_2 were plotted as a function of θ_H in Fig. 5 (dotted line). It is evident that the H(a) on Ru–Cs^+/MgO more effectively poisons the N_2 adsorption than on Ru/MgO. The molecular N_2 displacement rate on Ru–Cs^+/MgO was reduced from 11 μmolg^{-1} s^{-1} (θ_H=0) to 0.48 μmolg^{-1} s^{-1} (θ_H=14%) [Table 4(b)], but it was unable to be measured at θ_H=50% because the ν_{NN} peak intensity (θ_{N2}=1.3%) was too weak. The adsorption rates of N_2 at 183 K on H-free sample and that at θ_H=14% were 50 and 8.5 μmolg^{-1} s^{-1}, respectively [Table 4(b′)]. The decrease was more extensive (to 17%) than that (to 82%) on Ru/MgO [Table 2(b′)].

N_2 Isotope Equilibration and Ammonia Synthesis Reactions. The rates of isotope equilibration reaction of N_2 and ammonia synthesis reaction on Ru/MgO and Ru–Cs^+/MgO at 548 K are listed on Tables 2(c), (d) and 4(c), (d). The equilibration reaction rate on Ru–Cs^+/MgO was 8.8 times faster than on Ru/MgO, and the acceleration by doped Cs^+ was more evident in ammonia synthesis (16 times).

Hydrogen Spillover. In addition to on-top, bridging, and threefold H species on the Ru particle, an increase of broad peak around 3450 cm^{-1} was observed at 183—473 K (Fig. 2); this can be assigned to hydroxyl group bonded to lower-coordinated magnesium on MgO surface judging from the relatively lower wavenumber.[25,26] The initial growth rate of this peak increased as the increase of temperature in H_2, but the peak area was saturated (0.5—5 h) on the same level independent of the reaction temperature. The formed hydroxyl quantity corresponded to about three times that of surface Ru atoms. Hydrogen spillover rates at 183 K on Ru/MgO (1.9 μmolg^{-1} s^{-1}) and Ru–Cs^+/MgO (0.83 μmolg^{-1} s^{-1}) were far faster than N_2 isotope equilibration or ammonia synthesis at 548 K (Table 4), indicating that the H-spillover is faster equilibrium than steady state reaction rate in ammonia synthesis reaction.

Discussion

Hydrogen Adsorption. Three types of adsorbed hydrogen on Ru particles were detected for MgO-supported Ru catalysts by IR. The main peak at 1717 cm^{-1} and the shoulder weak peaks at 1880 and 1801 cm^{-1} were assigned as on-top, those at 1550 (ν_{as}) and 1330 (ν_s) cm^{-1} as bridging, and those at 1120 (ν_{as}) and 933 (ν_s) cm^{-1} as threefold species on Ru/MgO (183 K) based on H on single crystal, hydrido-complexes or clusters, and H on other supported metal catalysts. On Ru–Cs^+/MgO, the peak at 1781 cm^{-1} was assigned as on-top, those at 1540 (ν_{as}) and 1407 (ν_s) cm^{-1} as bridging, and those at 1233 (ν_{as}) and 940 (ν_s) cm^{-1} as threefold species (293 K). Each mode of on-top and bridging peaks had corresponding shifted peaks in D_2. The stability of bridging H (ca. 500 K in TPD) on Ru/MgO suggested hydrogen on the LC Ru sites. Chemisorbed amount of H on Ru/MgO corresponded one by one to surface Ru atoms, similar to $p(1\times1)$H on Ru(0001).[7]

The total peak areas for H(a) (θ_H) were 14, 36, and 65% after evacuation at 473, 293, and 183 K, respectively [Table 2(a)] on Ru/MgO. On Ru–Cs^+/MgO, the amounts of hydrogen chemisorbed were θ_H=14% at 373 K and 50% at 293 K. Only weak peaks were observed at 183 K in 6.7 kPa of H_2 [Fig. 6(a)] compared to the strong peak at 293 K [Fig. 6(b)]. This can be kinet-

ically explained by a slower dissociative adsorption of H_2 on Ru–Cs^+/MgO. The retardation of adsorption rate for H_2 by alkali metal dopant is known,[6,27] while the metal-H bond is stronger on such surfaces.[27] Indeed, our stretching frequency of on-top H (1781 cm^{-1}) on Ru–Cs^+/MgO was higher than that (1717 cm^{-1}) on Ru/MgO.

N_2 Adsorption. In H-free condition, the coverages of N_2 were 38 and 22% for Ru/MgO and Ru–Cs^+/MgO, respectively. The decrease of N_2 amount by doped Cs^+ was consistent with the long-range destabilization of N_2(a) by doped alkali metal.[6] Besides the effect of doped Cs^+, the decrease of θ_{N2} by H(a) was more drastic on Ru–Cs^+/MgO than on Ru/MgO, as seen from the initial decline of θ_{N2} as a function of θ_H in Fig. 5. By dual effects, long-range effect of Cs^+ and dipole effect of more negative H(a) enhanced by Cs^+, θ_{N2} became only 1.3—10% at θ_H=14—50% on Ru–Cs^+/MgO. Generally H bound to transition metal may be partially negatively charged, and N_2 bound to metal should coordinate through 5σ and 4σ to have partially positive charge,[6] consistent with our results. However, the wavenumber of ν_{NN} was shifted toward high position with the increase of θ_{N2} in Fig. 4, contrary to N_2 on Ru(0001) metal.[6] This suggests larger backdonation from Ru4d to $N_2 2\pi^*$; as a result, positive charge may not be so large for N_2 on Ru/MgO as on Ru metal. In line with this interpretation, the doped Cs^+ must donate more electron charge through Ru to both H and $N_2 2\pi^*$ on Ru–Cs^+/MgO. Doped Cs^+ ion has an enhanced dipole effect on H by making H(a) more negative and N_2(a) less positive.

The ν_{NN} wavenumber, first shifted toward lower-energy, suddenly changed the direction between θ_H=36 and 65% [Fig. 4(c), (d)]. In IR spectra the ν_{NN} peak was split to two peaks: original 2137 cm^{-1} and weaker shoulder peak at 2189 cm^{-1} at 65% of θ_H on Ru/MgO [Fig. 4(d)]. The blue-shifted peak at 2189 cm^{-1} can be explained to have stronger NN bonding by the repulsion with neighboring H(a) atoms. The wavenumber of ν_{NN} for adsorbed N_2 peak on Ru–Cs^+/MgO was not shifted [Table 3(b)], and N_2 was not adsorbed at high coverage of θ_H (over 50%) on Ru–Cs^+/MgO.

The Effect of H(a) on the Reactivity of N_2.
1. Ru/MgO. The rate of molecular N_2 isotope displacement reaction $^{15}N_2$(a)→$^{14}N_2$(a) on Ru/MgO was decreased to one tenth by less than 14% of H(a) [1.3 $\mu molg^{-1}s^{-1}$, Table 3(b)] compared to 11 $\mu molg^{-1}s^{-1}$ over the H-free surface. The population of adsorption style (on-top, bridging, threefold) for H is not known because each adsorption coefficient is difficult to estimate, but the H-free Ru atoms (H was not bound) when θ_H=14% should be 58—86%. As the θ_{N2} was 38% in this situation and the isotope displacement rate was unexpectedly slower on the surface with H(a), the ensemble area where N_2 displacement reaction does not occur should be the direct and nearest (and/or the next-nearest) Ru sites from H(a) on Ru/MgO. The adsorption rate of molecular N_2 was very fast either in H-free or H-adsorbed condition (θ_H=14%) on Ru/MgO [4—29 times faster than N_2 displacement rate; Table 2(b′)], and the N_2 displacement rate was proportional to P_{N2}. Based on this small decrease of adsorption rate of N_2 with the H adsorption (θ_H=14%), we believe that the contribution of long-range dipole effect of H to the N_2 displacement rate was small compared with the direct repulsion in the case of Ru/MgO.

The stability of bridging H in TPD experiment [Fig. 3(a)] implied that this species was bound on LC Ru site (edge site). At θ_H=14% most of the bridging H still remained (473 K), while only 0—9% of on-top or threefold site H remained (Fig. 3). It is often discussed whether the contribution of LC site to the metal catalysis is lower than that of the flat surface of metal particle. In this paper, the reaction rate of molecular N_2 displacement was followed not by the number of products formed, but directly by the number of adsorbed (intermediate) N_2 species on the relatively flat part and/or the LC part. If the LC sites were specifically active for this reaction and the displacement rate reduction to 14% was due to blocking of LC site by H(a), the ν_{NN} peak of N_2(a) would have shifted. If the "edge effect" existed in H-free condition, bare LC Ru would have influenced adsorbed N_2 to have a broader ν_{NN} peak than that at θ_H=14%. However, the wavenumbers of single peak in Fig. 4(a) and (b) were almost at the same position (2154 and 2153 cm^{-1}), and the peak was rather sharp in H-free condition. In this context, we believe that the participation of LC Ru site in N_2 displacement reaction was not so large. However, the possibility cannot be excluded that N_2 on LC Ru site and N_2 on relatively flat-part Ru site were in a fast equilibrium, one-sided toward the relatively flat-part site, and N_2 on relatively flat-part site was only observed by IR as an 'adsorbate pool', keeping the LC site as the real active site on Ru/MgO.

2. Ru–Cs^+/MgO. Compared to H-free condition, the rates of N_2 isotope displacement reaction in $^{14}N_2$ decreased drastically to 4% with a small amount of hydrogen adsorption (θ_H=14%) on Ru–Cs^+/MgO (Table 4), more serious than the rate decrease on Ru/MgO (5—12% at θ_H=14—65%) (Table 2). Fewer amount of N_2 (57%) can be adsorbed in H-free condition on Ru–Cs^+/MgO than on Ru/MgO (Tables 2 and 4) and one adsorbed H atom decreased the amount of N_2(a) more effectively on Ru–Cs^+/MgO than on Ru/MgO (Fig. 5, dotted line). The θ_{N2} was too low at θ_H=50% [1.3%, Table 4(a)] to measure the displacement rate. The N_2 displacement rates per θ_{N2} as a function of θ_H were plotted in Fig. 8 on Ru/MgO (solid line) and Ru–Cs^+/MgO (dotted line). Initially, the value was a little larger on Ru–Cs^+/MgO, but both decreased at H=14—65% reaching to the comparable value for Ru/MgO and Ru–Cs^+/MgO. The N_2 displacement rate per effective Ru

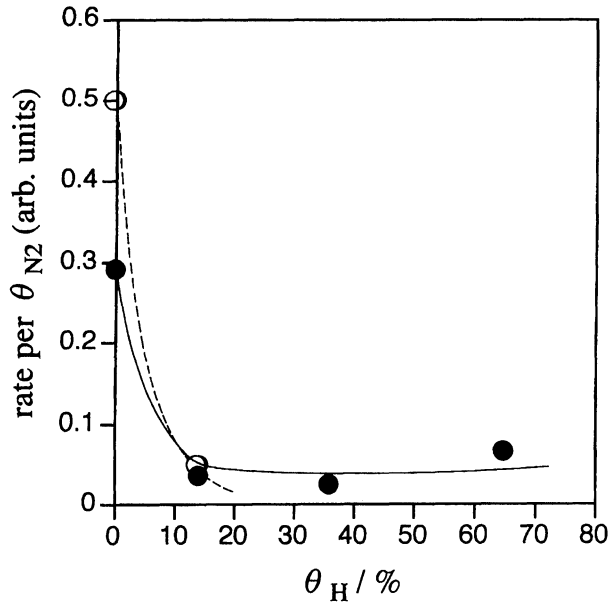

Fig. 8. The ratio of molecular N_2 exchange rate and θ_{N2} as a function of θ_H on Ru/MgO (solid line) and Ru–Cs^+/MgO (dotted line).

site (for N_2) for N_2 adsorption on Ru–Cs^+/MgO was supposed to be similar to Ru/MgO.

N_2 can be adsorbed on only 10% of surface Ru sites, when hydrogen is adsorbed ($\theta_H=14\%$). By the same estimation, H-free Ru sites would be 58—86% when $\theta_H=14\%$ also on Ru–Cs^+/MgO. Therefore, H(a) on Ru–Cs^+/MgO prevented N_2 from being adsorbed on a larger Ru region that Ru/MgO. In this situation, the direct interaction of H with N_2 molecules is improbable on Ru/MgO. Instead, long-range dipole effect of H enhanced by doped Cs^+ decreased the displacement rate of N_2 in the case of Ru–Cs^+/MgO.

Relevance to Catalysis. Although the rates of molecular N_2 isotope displacement reaction on Ru/MgO and Ru–Cs^+/MgO were the same, the acceleration of N_2 equilibration reaction in H-free catalyst and of ammonia synthesis reaction were quite extensive (8.8 and 16 times, respectively) [Tables 2(c), (d) and 4(c), (d)]. Though it was difficult to correlate these rates with IR data for H(a) because of the higher reaction temperature in the catalysis (548 K), these two reactions were known to be retarded by H(a).[2,17—19,21] As discussed previously, the molecular N_2 displacement reaction was prohibited on the nearest Ru atoms to H(a) on Ru/MgO. The prohibited area with H(a) becomes wider on Ru–Cs^+/MgO through the dipole effect. As the rate-limiting N_2 dissociation step in N_2 equilibration reaction or ammonia synthesis reaction demands (more than) two Ru atoms to interact N_2 through $N_2 1\pi$,[2,3] the effects of H(a) and Cs^+ studied here may not be applied to the catalysis directly. Nevertheless, the decrease of θ_{N2} by doped Cs^+ and also by enhanced dipole effect of H(a) should also be considered for further developments of Ru catalysts for catalysis at elevated pressures where the poison of H(a) should be more serious on Ru–Cs^+/MgO.

The increase of NH_3 formation rates was observed (2—4 times) on $[Ru_3(\mu\text{-}O_s)_3]$-derived clusters on CeO_2 or on Ni-doped CeO_2 when the total pressure was varied from 10^2 to 10^3 kPa. Corresponding to this pressure dependency, only very weak H adsorption compared to Ru–Cs^+/MgO was observed on these catalysts around 10^2 kPa in IR, suggesting the IR study for H(a) and reactivities of N_2 on partially H(a)-covered surface is closely related to NH_3 formation activity. This relation between weak H(a) and positive pressure dependency for the N_2–H_2 reaction on $[Ru_3(\mu\text{-}O_s)_3]$(-Ni)/CeO_2 will be reported in a separate paper.[20]

Conclusion

(1) We observed the hydrogen to be dissociatively adsorbed at on-top, bridging, and threefold sites on Ru/MgO and Ru–Cs^+/MgO by FTIR. The bridging site H(a) on Ru/MgO, quite stable in TPD (ca. 500 K), was suggested to be on a low-coordination Ru site such as the edge site.

(2) The area where the adsorption of N_2 was inhibited was wider in the presence of Cs^+. This difference can be interpreted as the direct effects of Cs^+ and negative charge donation from Cs^+ to H and $N_2 2\pi^*$ through Ru to enhance the long-range dipole effect of H(a).

(3) The molecular N_2 displacement rate became slower in the order on Ru/MgO and Ru–Cs^+/MgO by the existence of a small amount of hydrogen ($\theta_H=14\%$). The main factors of this decrease were suggested to be the direct repulsion of N_2 and H on Ru/MgO and indirect dipole effect of H(a) enhanced by doped Cs^+ on Ru–Cs^+/MgO.

References

1) "Vibrational Spectroscopy on Molecules on Surfaces," ed by J. T. Yates, Jr., and T. E. Madey, Plenum Press, New York (1987).

2) A. Ozaki and K. Aika, "Catalysis- Science and Technology," ed by J. R. Anderson and M. Boudart, Springer-Verlag, Berlin (1981), Vol. 1, p. 87.

3) S. R. Tennison, "Catalytic Ammonia Synthesis, Fundamentals and Practice," ed by J. R. Jennings, Plenum Press, New York (1991), p. 303.

4) F. Fisher and H. Tropsch, *Brennst. Chem.*, **7**, 97 (1926).

5) Y. Fukuoka, H. Nagahara, and M. Konishi, *Syokubai* (*Japanese*), **35**, 34 (1993).

6) R. A. de Paola, F. M. Hoffmann, D. Heskett, and E. W. Plummer, *Phys. Rev. B*, **35**, 4236 (1987).

7) M. Sokolowski, T. Koch, and H. Pfnür, *Surf. Sci.*, **243**, 261 (1991).

8) H. Pfnür, P. Feulner, and D. Menzel, *J. Chem. Phys.*, **79**, 4613 (1983).

9) T. Sasaki, T. Aruga, H. Kuroda, and Y. Iwasawa, *Surf. Sci.*, **240**, 223 (1990).

10) G. Held, H. Pfnür, and D. Menzel, *Surf. Sci.*, **271**, 21

(1992).
11) P. Feulner and D. Menzel, *Surf. Sci.*, **154**, 465 (1985).
12) P. Hofmann and D. Menzel, *Surf. Sci.*, **152/153**, 382 (1985).
13) M. A. Barteau, J. Q. Broughton, and D. Menzel, *Surf. Sci.*, **133**, 443 (1983).
14) H. Conrad, R. Scala, W. Stenzel, and R. J. Unwin, *J. Chem. Phys.*, **81**, 6371 (1984).
15) J. T. Yates, Jr., C. H. F. Peden, J. E. Houston, and D. W. Goodman, *Surf. Sci.*, **160**, 37 (1985).
16) H. Shi and K. Jacobi, *Surf. Sci.*, **278**, 281 (1992), and the references therein.
17) T. Hikita, Y. Kadowaki, and K. Aika, *J. Phys. Chem.*, **95**, 9396 (1991).
18) K. Aika, M. Kumasaka, T. Oma, O. Kato, H. Matsuda, N. Watanabe, K. Yamazaki, A. Ozaki, and T. Onishi, *Appl. Catal.*, **28**, 57 (1986).
19) Y. Kadowaki, S. Murata, and K. Aika, *Syokubai* (*Japanese*), **33**, 380 (1991).
20) Y. Izumi and K. Aika, to be published.
21) K. Aika, T. Takano, and S. Murata, *J. Catal.*, **136**, 126 (1992).
22) J. Kubota and K. Aika, *J. Chem. Soc., Chem. Commun.*, **1992**, 661.
23) J. Kubota and K. Aika, *J. Chem. Soc., Chem. Commun.*, **1991**, 1544.
24) "Infrared and Raman Spectra of Inorganic and Coordination Compounds," ed by K. Nakamoto, Wiley, London (1978).
25) H. D. Kaesz and R. B. Saillant, *Chem. Rev.*, **72**, 231 (1972).
26) H. Zhang and G. L. Schrader, *J. Catal.*, **99**, 461 (1986).
27) Y. Iwasawa, *Adv. Catal.*, **35**, 187 (1987).
28) J. P. Wey, W. C. Neely, and S. D. Worley, *J. Phys. Chem.*, **95**, 8881 (1991).
29) N. K. Kavtaradze and N. P. Sokolova, *Russ. J. Phys. Chem.*, **44**, 1485 (1970).
30) J. A. Andrews, U. A. Jayasooriya, I. A. Oxton, D. B. Powell, N. Sheppard, P. F. Jackson, B. F. G. Johnson, and J. Lewis, *Inorg. Chem.*, **19**, 3033 (1980).
31) K. Christmann, *Surf. Sci. Rep.*, **9**, 1 (1988).
32) A. M. Baró, H. Ibach, and H. D. Bruchmann, *Surf. Sci.*, **88**, 384 (1979).
33) S. A. R. Knox, J. W. Koepke, M. A. Andrews, and H. D. Kaesz, *J. Am. Chem. Soc.*, **97**, 3942 (1975).
34) E. Knözinger, K. Jacob, and P. Hofmann, *J. Chem. Soc., Faraday Trans.*, **89**, 1101 (1993).
35) T. Shido, K. Asakura, and Y. Iwasawa, *J. Chem. Soc., Faraday Trans. 1*, **85**, 441 (1989).
36) C. Resch, V. Zhukov, A. Lugstein, H. F. Berger, A. Winkler, and K. D. Rendulic, *Chem. Phys.*, **177**, 421 (1993).